Doppler seismology

with a Michelson Interferometer

J.P. Maillard[1], B. Mosser[2]

1 Institut d’Astrophysique de Paris (CNRS)
2 LESIA, Observatoire de Paris, Meudon

CONTENTS

1. **Specifications for a ground-based stellar seismometer**

CONTENTS

CONTENTS

1. **Specifications for a ground-based stellar seismometer**
2. **Seismometry in the Fourier space**
3. **Simulations of the fundamental performances of a FT seismometer**

CONTENTS

1. **Specifications for a ground-based stellar seismometer**
2. **Seismometry in the Fourier space**
3. **Simulations of the fundamental performances of a FT seismometer**
4. **Results of simulations**

CONTENTS

Detection of p-modes

Two methods:

- by photometry

The stellar oscillations generate temperature pulsations.

Repeated recording of the visible photometry of a star:

$\sim$ every min, over several days

Precision required: 10^{-6}

$\Rightarrow$ Measurements with time of photometric micro-variations

Only feasible from space

Space missions dedicated to asteroseismology:

MONS, MOST, COROT

Detection of p-modes

Two methods:

- by spectroscopy

The stellar oscillations generate surface motions.

Repeated recording of a high-resolution, visible spectrum of a star: $\sim$ every min, over several days

$\Rightarrow$ Measurements with time of small Doppler shifts (after subtraction of the mean radial velocity)

Feasible from ground

Need to set up a worldwide network of dedicated, échelle spectrometers

Specifications of a ground-based grating spectrometer dedicated to asteroseismology:

- high spectral resolution $\sim 10^5$
- broad spectral coverage *visible range*

a fiber-fed cross-dispersed échelle spectrometer

- high stability *temperature control* $\sim 10^{-2}$ *K*
- spectral reference 10^{-9}
- minimum number of instruments for a network 3

Specifications of a ground-based grating spectrometer dedicated to asteroseismology:

- high spectral resolution $\sim 10^5$
- broad spectral coverage *visible range*

a fiber-fed cross-dispersed échelle spectrometer

- high stability *temperature control* $\sim 10^{-2}$ *K*
- spectral reference 10^{-9}
- minimum number of instruments for a network 3

Another approach: with a Michelson interferometer

Seismometry in the Fourier space

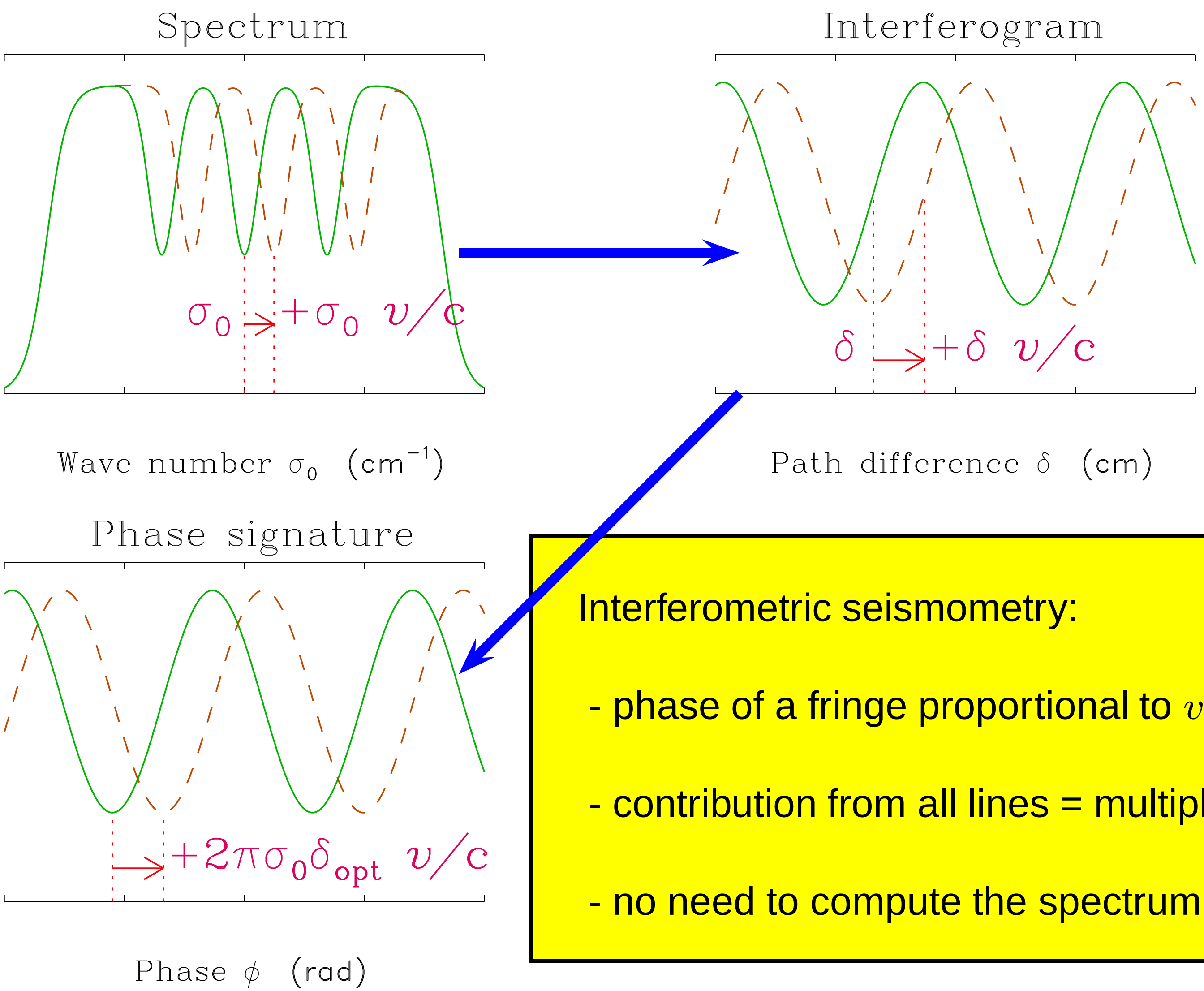

Interferometric seismometry:

- phase of a fringe proportional to v
- contribution from all lines = multiplex advantage
- no need to compute the spectrum

What OPD to use?

Interferogram $I(\delta)$ of a single absorption line at σ_0, depth A_0, visibility function $\Gamma(\delta)$:

$$I(\delta) = A_0\,\Gamma(\delta)\,\cos\,2\pi\sigma_0\delta$$

Modulation of the output signal by Doppler velocity dv:

$$\mathrm{d}I(\delta) = 2\pi\frac{\sigma_0}{c}\,A_0\,\delta\Gamma(\delta)\,\sin\,2\pi\sigma_0\delta\mathrm{d}v$$

Maximum signal at δ_0 = zero crossing of a fringe (sinus = 1)

$$\boxed{\mathrm{d}I(\delta_0) = 2\pi\frac{\sigma_0}{c}A_0\color{red}{\boldsymbol{\delta_0\Gamma}(\boldsymbol{\delta_0})}\,\mathrm{d}v}$$

What OPD to use?

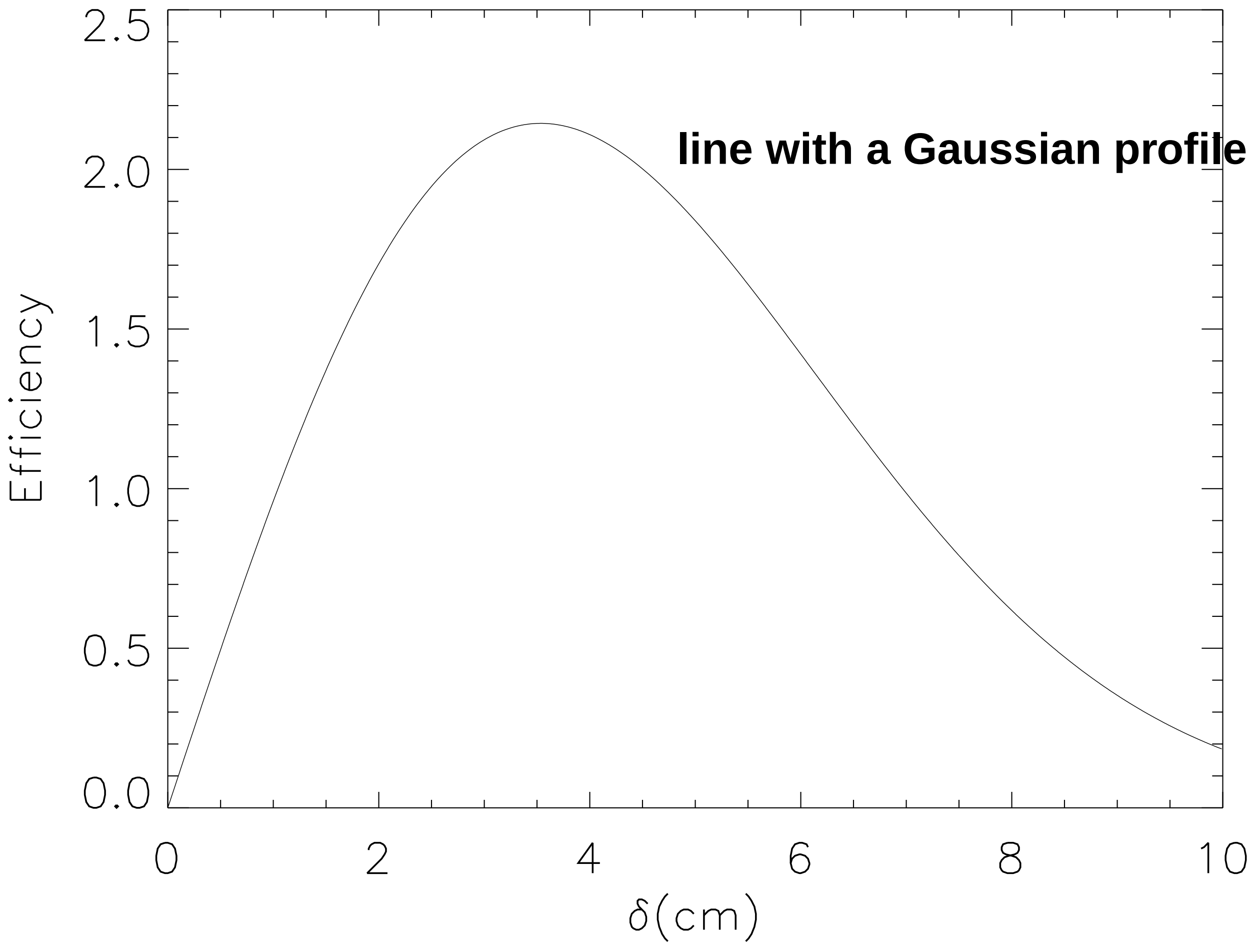

$\delta \times \Gamma(\delta)$ = Efficiency fonction

Selection of the optimum OPD

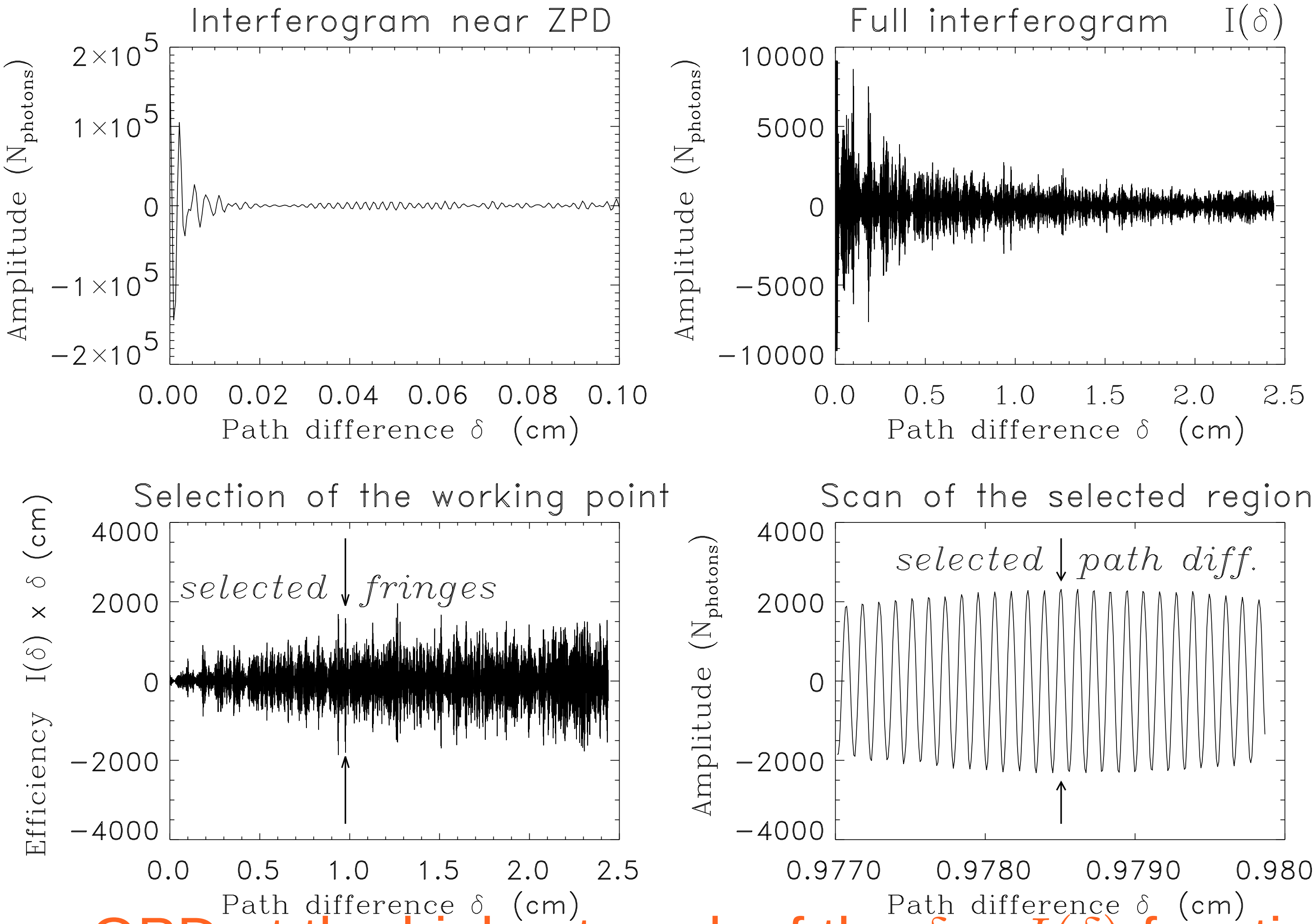

Optimum OPD at the highest peak of the $\delta \times I(\delta)$ function

From observations with the CFHT-FTS: *(Mosser, Maillard et al. 2000, Icarus, 144, 104).*

Data acquisition (1)

In principle, simply with the interferometer blocked at δ_{opt}, on a fringe zero-crossing, recording of the oscillation signal on the linear part of the selected fringe:

– Sensitive to the scintillation noise

– Sensitive to the transparency fluctuations

– Sensitive to the drifts of OPD (no velocity detection at the peak of a fringe)

Solution: the recording of a phase signal

Data acquisition (2)

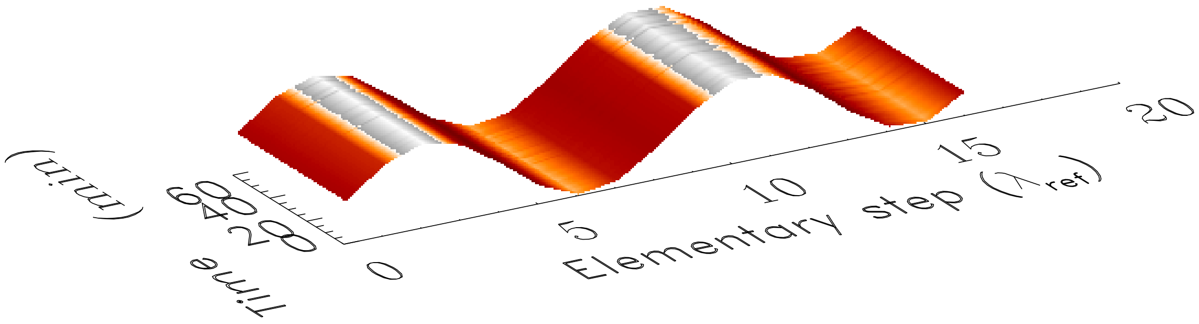

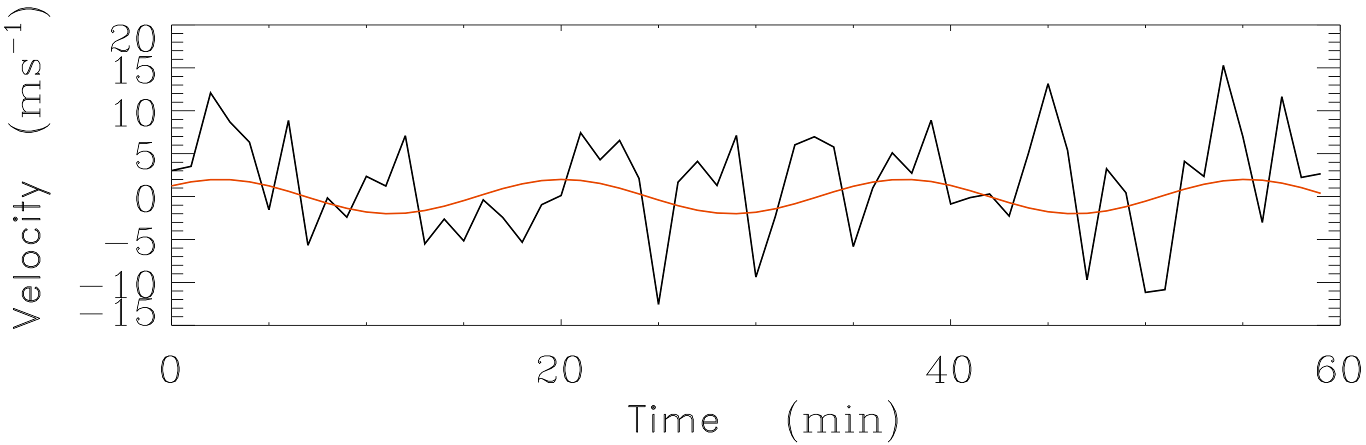

Continuous step-by-step scanning of the same fringe. Fitting of a sinewave through the recorded samples (minimum 3)

Fundamental performances

Simulations:

from synthetic spectra of dwarf stars: T_{eff} *5000 to 7000K*

range: *380 - 680 nm (14700 - 26300 cm^{-1})*

Parameters:

V magnitude: *0 to 6*

rotational velocity $vsini$: *0 to 80 km s^{-1}*

Conditions:

2-m class telescope

photon noise-limited by the star flux

MAIN RESULTS OF SIMULATIONS

- Comparison of two intrument configurations
  - unique narrow-band spectral domain: two detectors **FS1**
  - multi-bandpass, by post-dispersion: array detectors **FSλ**

Photon noise-limited Doppler measurements with a Fourier Transform Seismometer I. Fundamental Performances
Mosser, B., Maillard, J.P., & Bouchy, F., PASP, 115, 990-1001, (2003)

MAIN RESULTS OF SIMULATIONS

- Comparison of two intrument configurations
  - unique narrow-band spectral domain: two detectors **FS1**
  - multi-bandpass, by post-dispersion: array detectors **FSλ**
- Determination of the useful spectral range

Photon noise-limited Doppler measurements with a Fourier Transform Seismometer I. Fundamental Performances
Mosser, B., Maillard, J.P., & Bouchy, F., PASP, 115, 990-1001, (2003)

MAIN RESULTS OF SIMULATIONS

- Comparison of two intrument configurations
  - – unique narrow-band spectral domain: two detectors **FS1**
  - – multi-bandpass, by post-dispersion: array detectors **FSλ**
- Determination of the useful spectral range
- Determination of the optimum OPD

Photon noise-limited Doppler measurements with a Fourier Transform Seismometer I. Fundamental Performances
Mosser, B., Maillard, J.P., & Bouchy, F., PASP, 115, 990-1001, (2003)

MAIN RESULTS OF SIMULATIONS

- Comparison of two intrument configurations
  - unique narrow-band spectral domain: two detectors **FS1**
  - multi-bandpass, by post-dispersion: array detectors **FSλ**
- Determination of the useful spectral range
- Determination of the optimum OPD
- Influence of the stellar $v sin i$

Photon noise-limited Doppler measurements with a Fourier Transform Seismometer I. Fundamental Performances
Mosser, B., Maillard, J.P., & Bouchy, F., PASP, 115, 990-1001, (2003)

MAIN RESULTS OF SIMULATIONS

- Comparison of two intrument configurations
  - – unique narrow-band spectral domain: two detectors **FS1**
  - – multi-bandpass, by post-dispersion: array detectors **FSλ**
- Determination of the useful spectral range
- Determination of the optimum OPD
- Influence of the stellar $v sin i$
- Comparison with a grating spectrometer

Photon noise-limited Doppler measurements with a Fourier Transform Seismometer I. Fundamental Performances
Mosser, B., Maillard, J.P., & Bouchy, F., PASP, 115, 990-1001, (2003)

Spectral domain

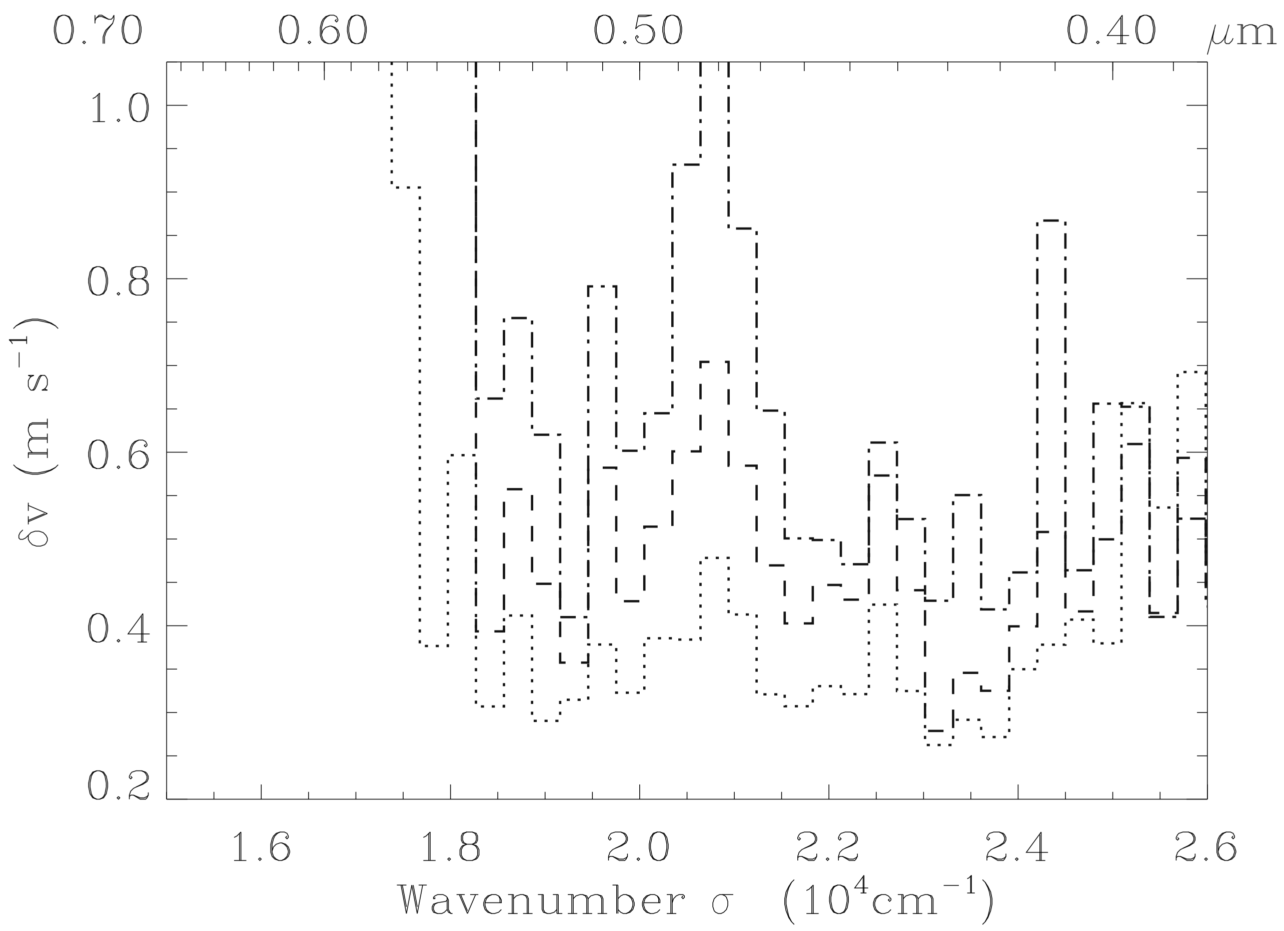

Limit of velocity detection (δv) due to photon noise as a function of the mean λ of the bandpass for three different dwarf stars (*dot* K2, *dash* F9, *dot-dash* F2).

Conclusion: combined with CCD efficiency $\Rightarrow$ 400 – 560 nm

Comparison of the two configurations

– two detectors, unique narrow-band spectral domain **FS1**

Mode tested with the CFHT-FTS on stars and on Jupiter

– array detectors, multi-bandpass by post-dispersion **FSλ**

Obtained by a low-resolution grating on each parallel, output beam of the interferometer (dual output)

Target	mag	vsini km s^{-1}	FS1 δv cm s^{-1}	FSλ $< \delta v >$ cm s^{-1}	$\delta v_{\mathrm{FS1}}/\delta v_{\mathrm{FS}\lambda}$
F3V	6.3	12.3	51	17.1	**3.0**
F7V	5.0	11.2	23	7.6	**3.0**
G0V	4.8	10.9	19	5.7	**3.3**
G5V	5.4	10.8	18	5.7	**3.2**
K3V	6.2	12.5	17	5.7	**3.0**

Comparison of the two configurations

Conclusions:

– Multi-bandpass better by a factor ~ 3 than the mono-bandpass configuration.

– Gain by the coverage of a large spectral range, without increasing the photon noise.

Necessary to adopt a montage with a post-disperser

Optimum OPD versus $v \sin i$

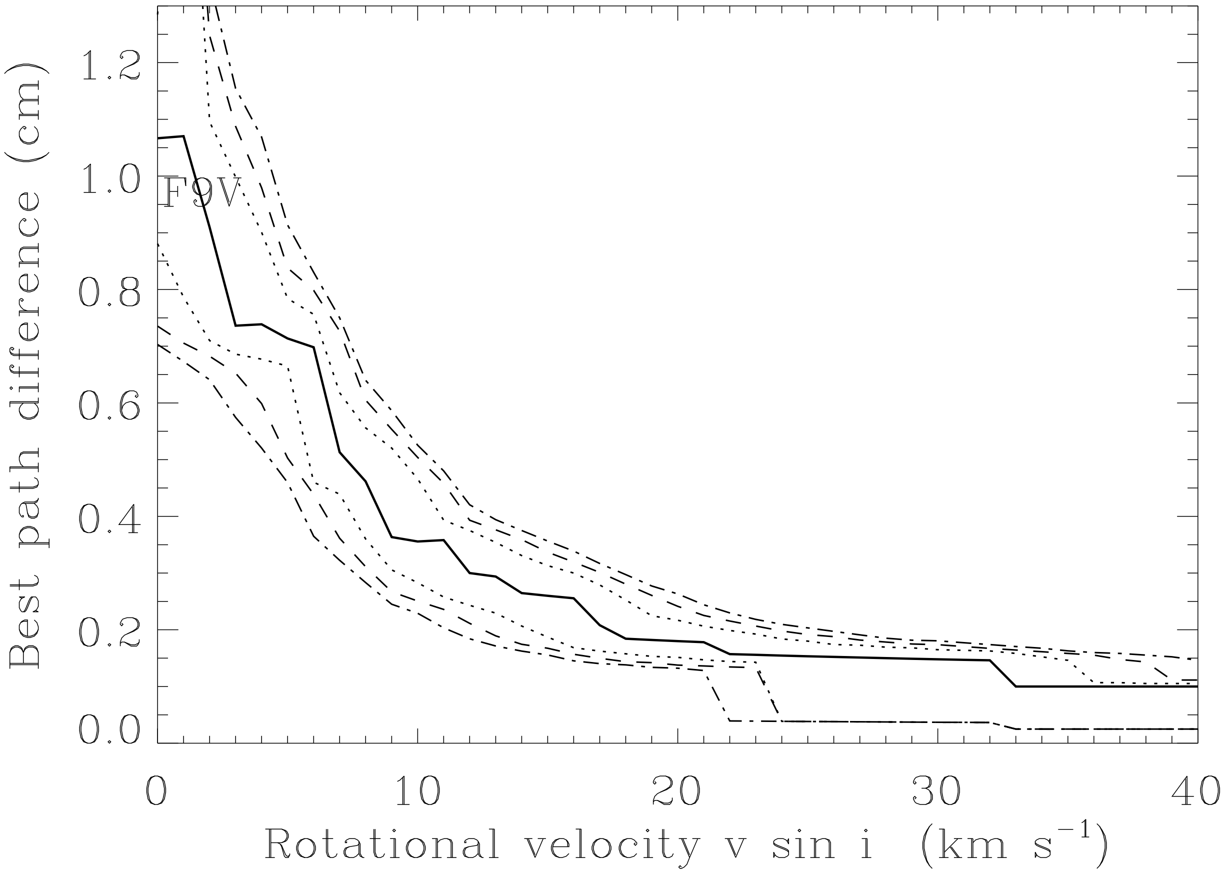

Best OPD as a function of $v sin i$ for a F9V star (——). Reduction of performances by 5% (*dot*), 10% (*dash*) and 15% (*dot-dash*).

Optimum OPD versus $v \sin i$

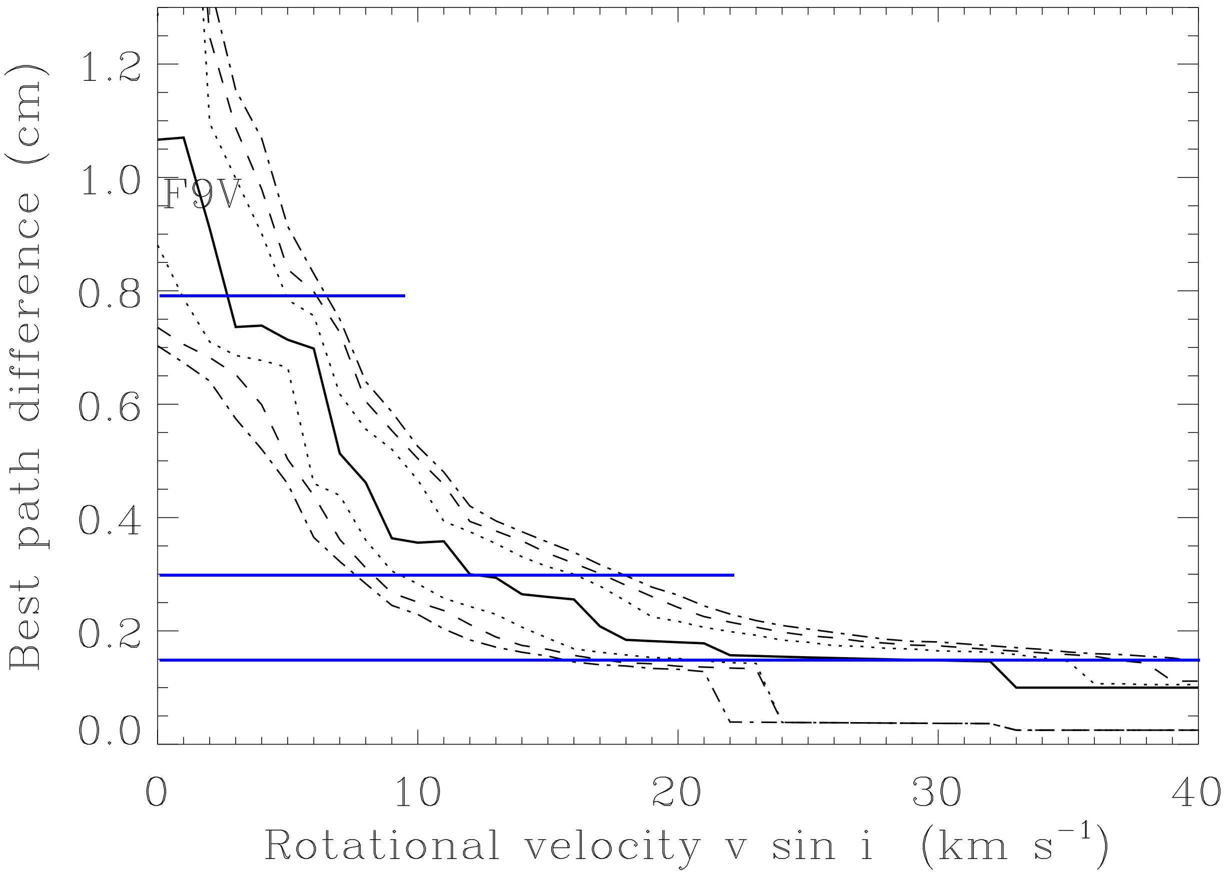

Conclusion: to cover the full range of $vsini$

3 OPDs needed, 0.8cm, 0.3cm, 0.15cm

Influence of post-disperser resolution

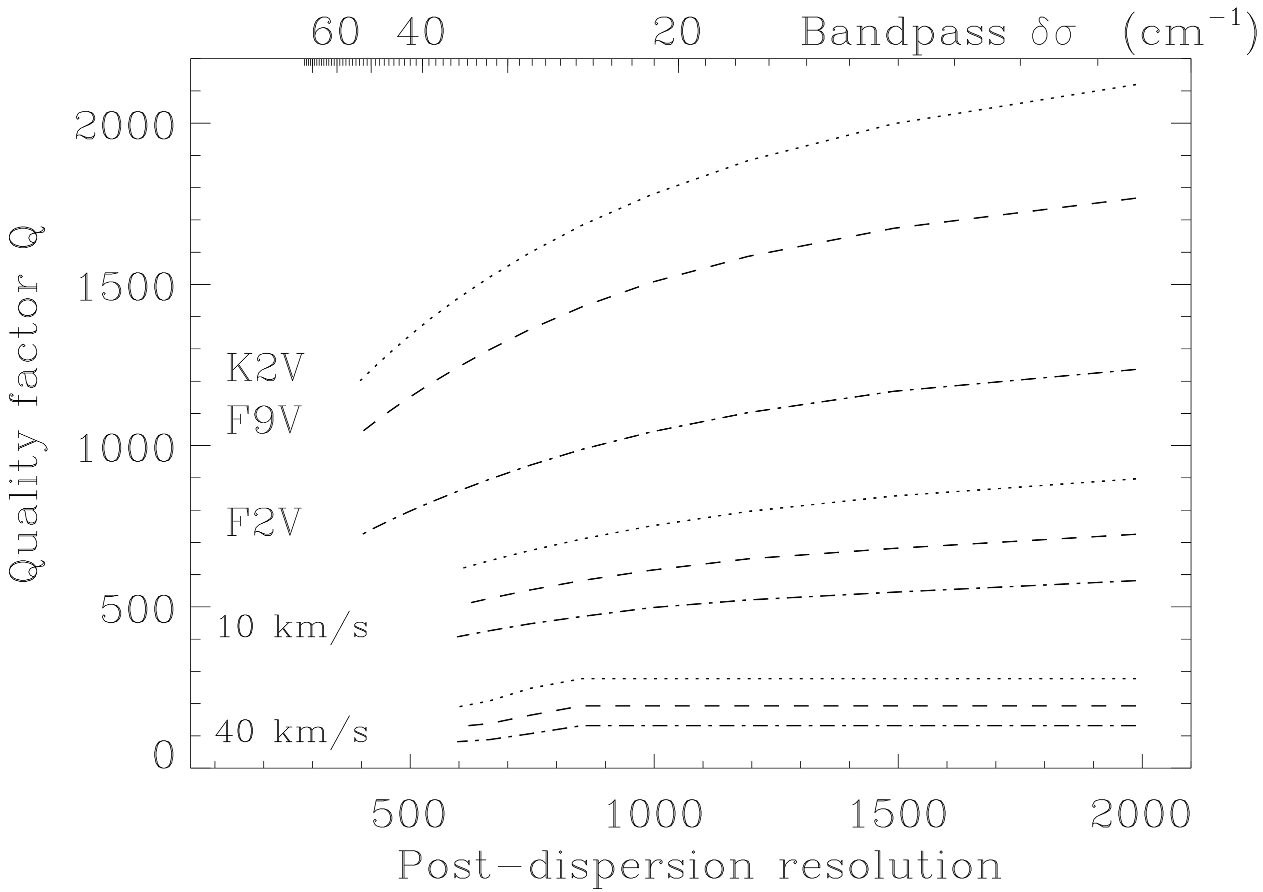

Quality factor of the stellar spectrum as a function of the resolution of the post-disperser for $v sini$ = 0, 10 and 40 km s^{-1} and 3 stellar types K2V (*dot*), F9V (*dash*) and F2V (*dash-dot*)

Influence of post-disperser resolution

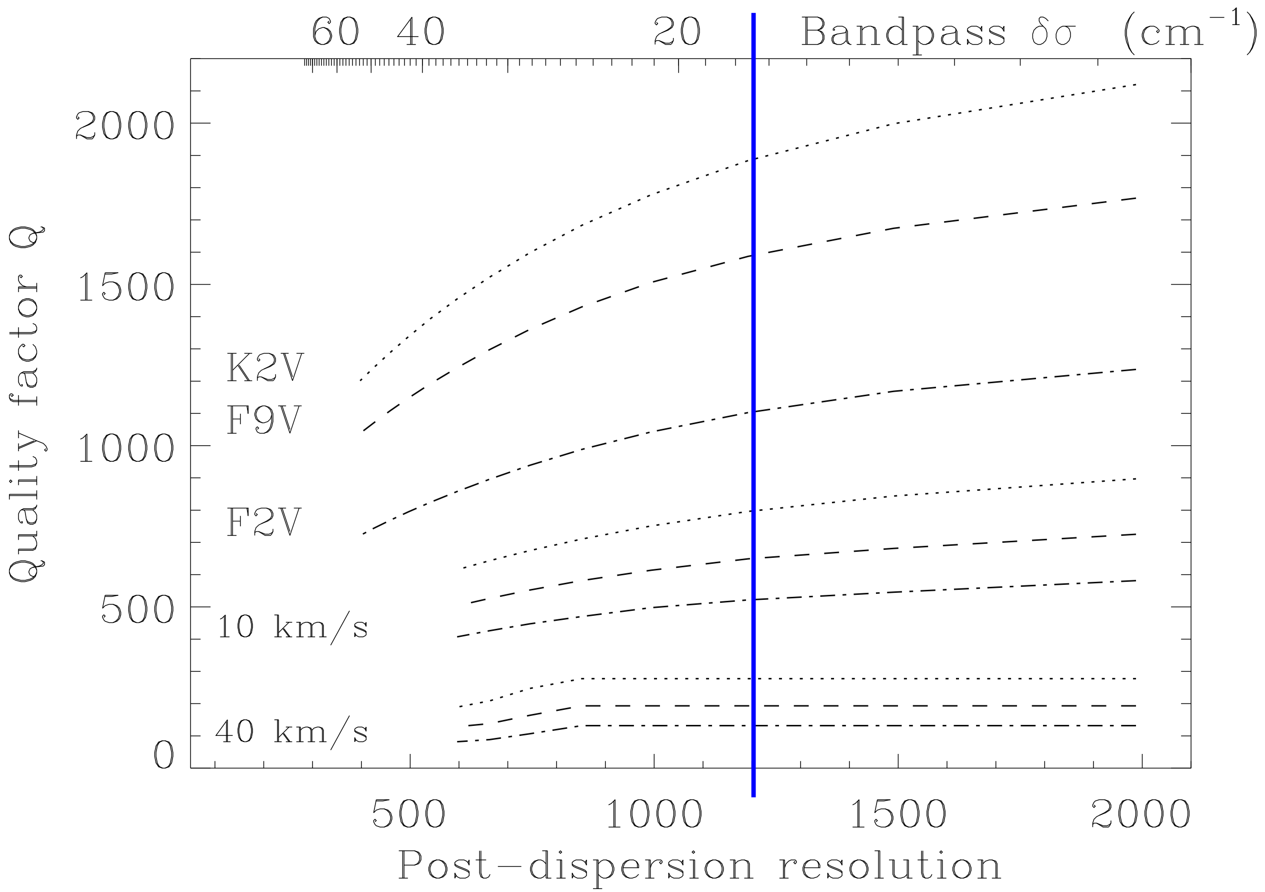

Quality factor of the stellar spectrum as a function of the resolution of the post-disperser for $vsini$ = 0, 10 and 40 km s^{-1} and 3 stellar types K2V (*dot*), F9V (*dash*) and F2V (*dash-dot*)

Conclusion: resolution of post-disperser ⇒ 1200

Influence of $vsini$ on performances

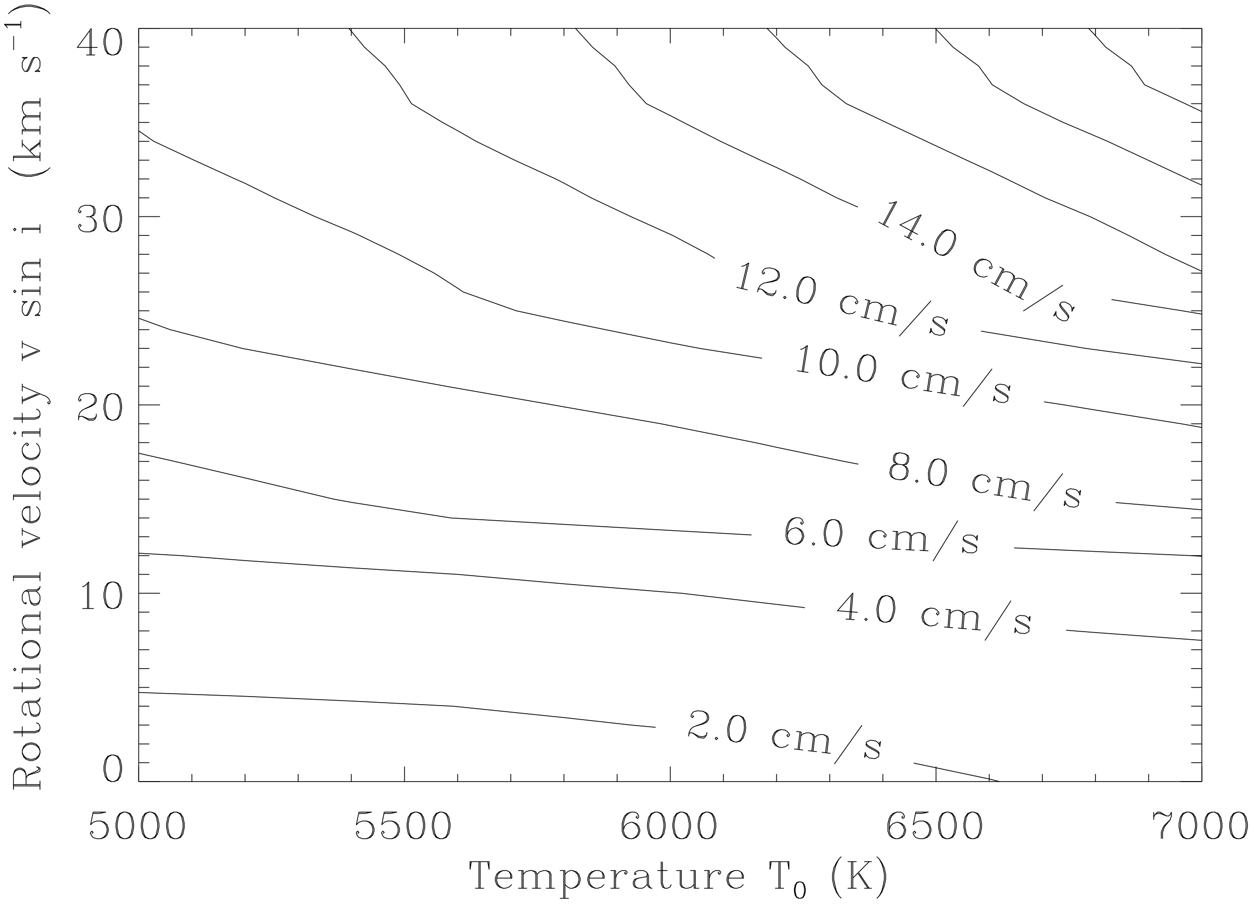

δv_{rms} as a function of effective stellar T_0 and $v \sin i$

Comparison with a grating spect. (GS)

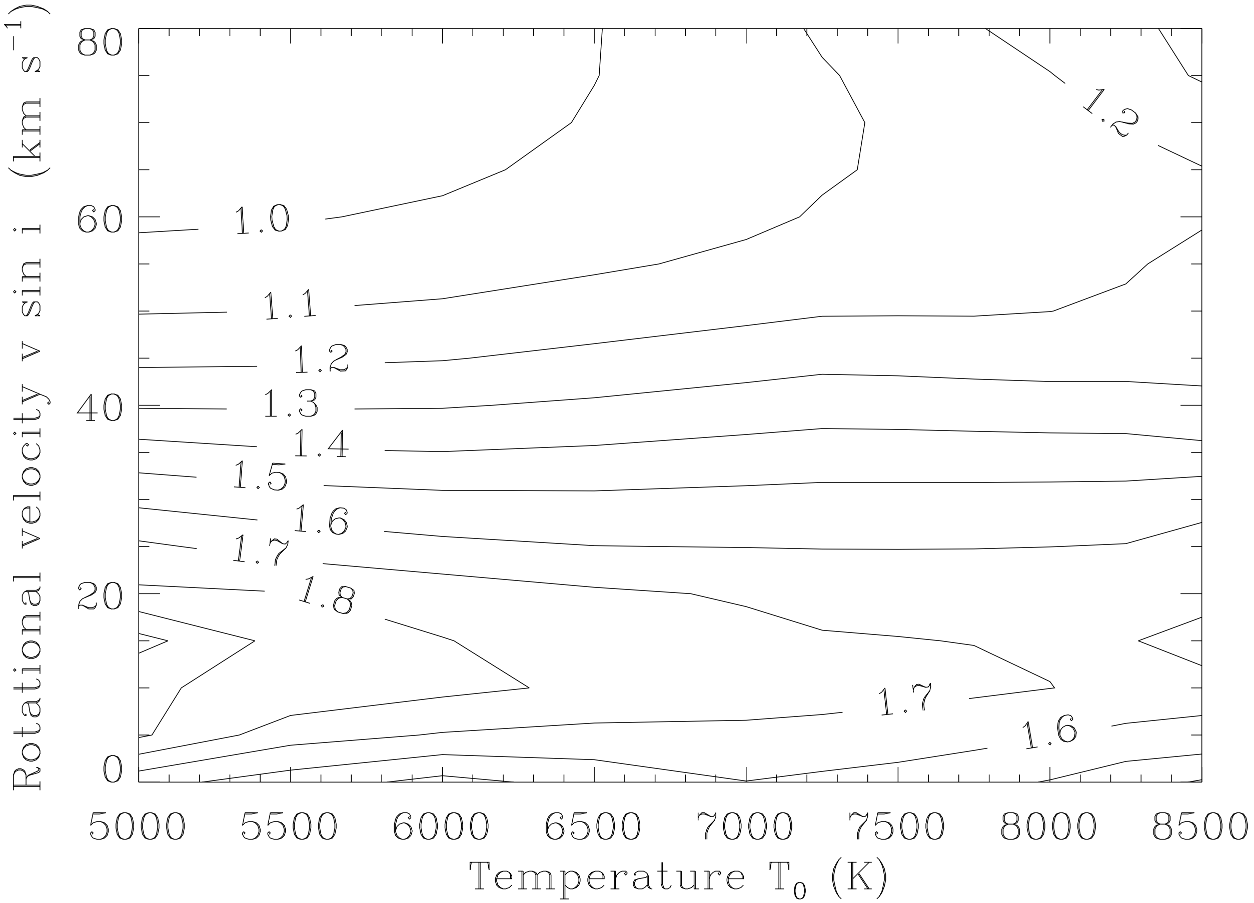

Ratio of the performances of $\delta v_{\mathrm{FTS}}/\delta v_{\mathrm{GS}}$ as a function of T$_0$ and $vsini$ on the **same star**, for the **same observing conditions** ($R_{\mathrm{GS}} = 88\,000$, $R_{post-disp} = 1200$).

Conclusion: FTS < GS by a factor between 1 and 1.8

The SIAMOIS concept

stands in French for:

Sismomètre Interferentiel A Mesurer *les* Oscillations Stellaires

The SIAMOIS concept

stands in French for:

Sismomètre Interferentiel A Mesurer *les* Oscillations Stellaires

All the results of the simulations used to define the characteristics of a FTS dedicated to asteroseismology

The SIAMOIS concept

stands in French for:

Sismomètre Interferentiel A Mesurer *les* Oscillations Stellaires

All the results of the simulations used to define the characteristics of a FTS dedicated to asteroseismology

- high stability *no adjustment*
- simplicity *no servo-system, no electronics control*
- no scanning *all samples recorded simultaneously*
- modest size *small path difference*
- adaptable to Dome C conditions

A monolithic interferometer, with no moving parts

Schematic diagram of SIAMOIS

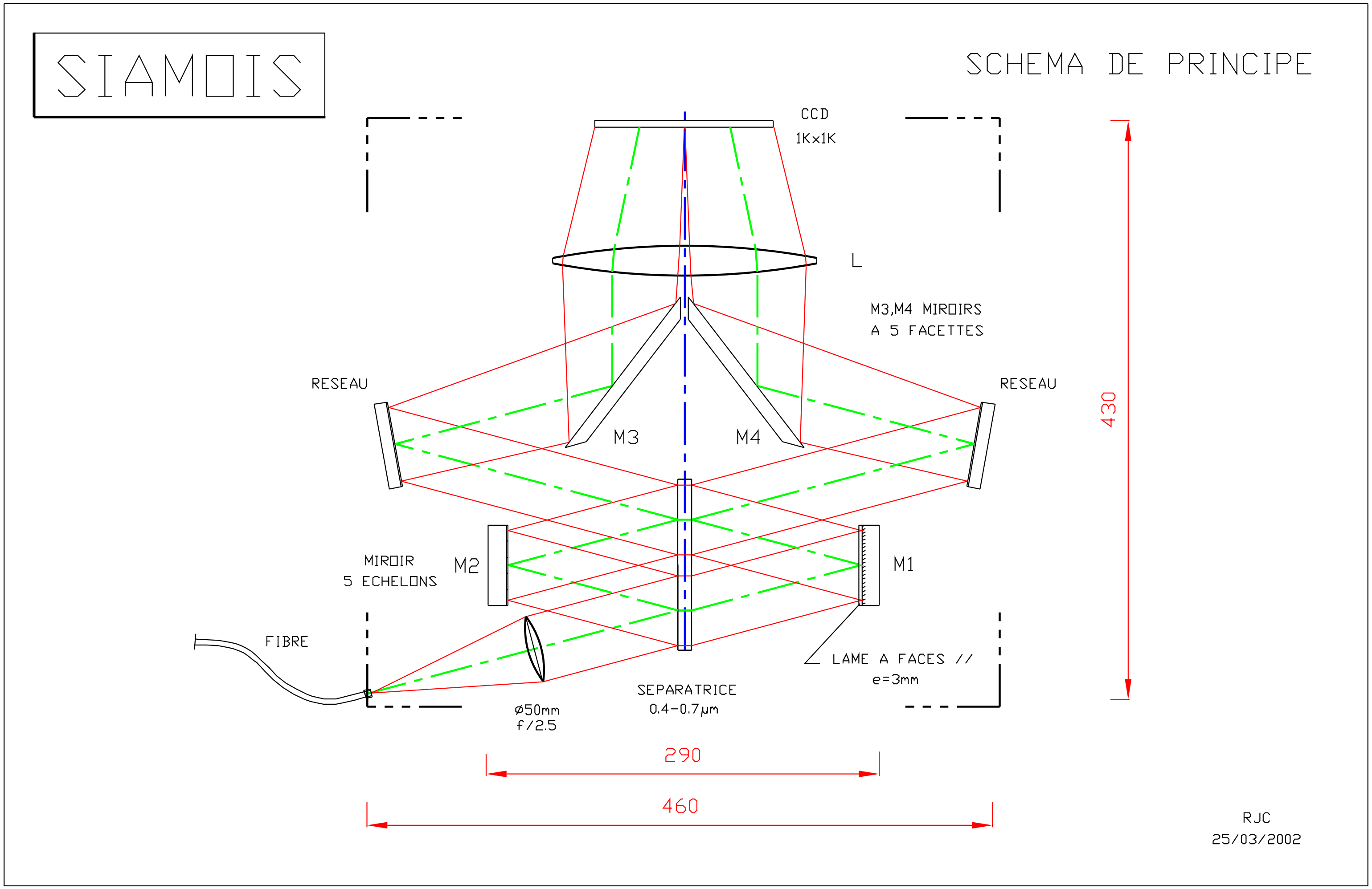

The concept is based on a compact Mach-Zehnder interferometer:
a single beamsplitter and two output beams

Elements of the SIAMOIS design

- feeding of the instrument from the telescope by optical fiber

  stabilization of star image

- fixed OPD — a parallel plate in one arm
- sampling of a fringe — in 5 points
- one mirror of the interferometer — 5 steps of depth = $\lambda_{mean}/10$

Elements of the SIAMOIS design

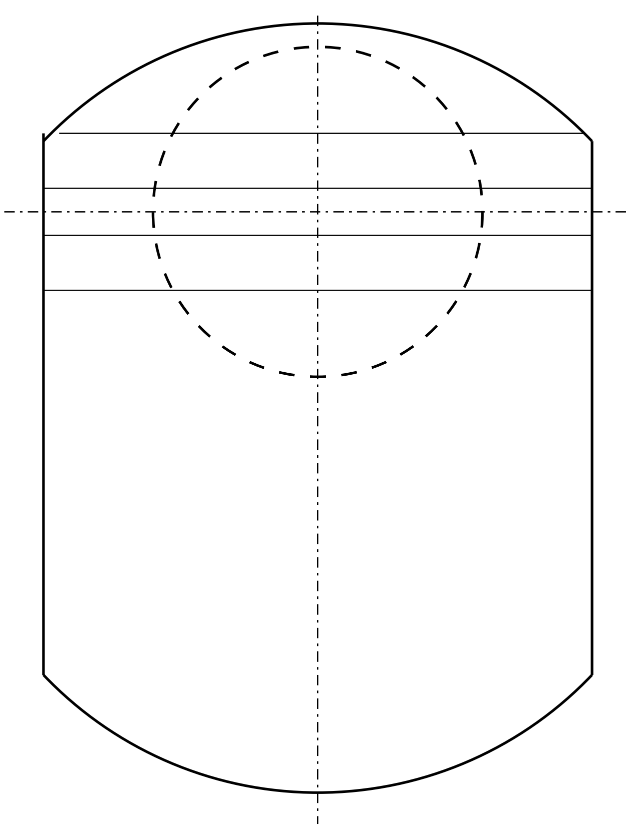

Profile of the 5-step mirror. Depth of each step $\lambda_{mean}/10$. Width of each portion of the beam calculated to obtain about 5 equal intensity channels

Elements of the SIAMOIS design

- feeding of the instrument from the telescope by optical fiber

  stabilization of star image
- fixed OPD — a parallel plate in one arm
- sampling of a fringe — in 5 points
- one mirror of the interferometer — 5 steps of depth = $\lambda_{mean}/10$
- two beam slicer mirrors — 5 channels
- post-dispersion by two low-resolution gratings — R=1200
- a blue CCD — 1024$\times$256

A monolithic interferometer

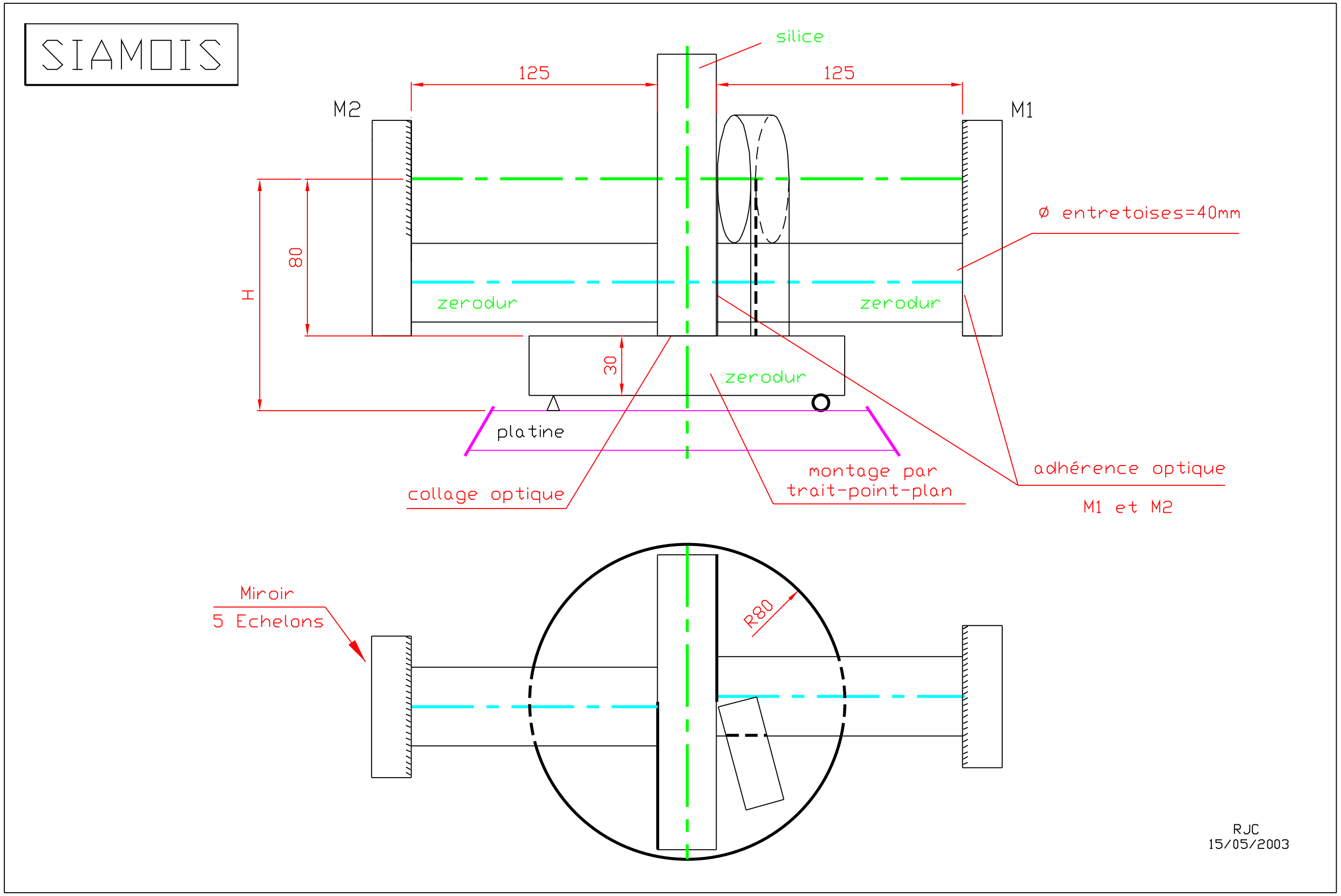

Fig. 3 Ensemble interférométrique monolithique avec miroirs et séparatrice.
Montage de la lame à faces parallèles.

The two mirrors and the beamsplitter make a single optical block with two Zerodur cylindrical spacers optically contacted. The block is bonded on the optical bench.

A monolithic interferometer

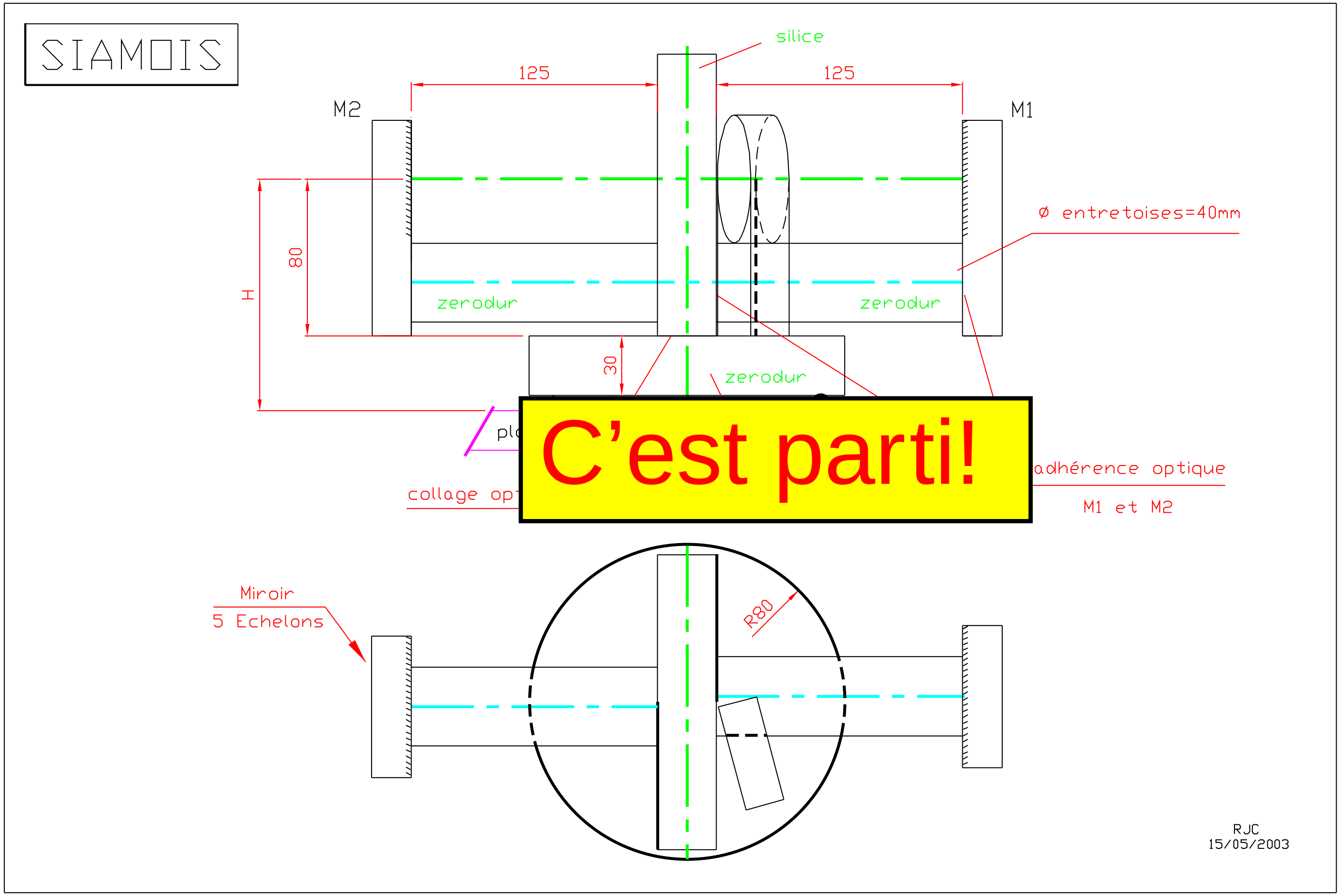

C’est parti!

Fig. 3 Ensemble interférométrique monolithique avec miroirs et séparatrice.
Montage de la lame à faces parallèles.

The two mirrors and the beamsplitter make a single optical block with two Zerodur cylindrical spacers optically contacted. The block is bonded on the optical bench.